Synthesis and Characterization of Poly(dimethylsiloxane-urethane) Nanocomposites: Effect of (In)Completely Condensed Silsesquioxanes on Thermal, Morphological, and Mechanical Properties

K. Madhavan, D. Gnanasekaran, B. S. R. Reddy

Industrial Chemistry Laboratory, Central Leather Research Institute, Chennai 600 020, Tamil Nadu, India

Received 22 April 2008; accepted 21 December 2008
DOI 10.1002/app.29943
Published online 17 August 2009 in Wiley InterScience (www.interscience.wiley.com).

ABSTRACT: The structural properties of completely condensed and incompletely condensed silsesquioxane in the polyurethane nanocomposites containing 17.5 wt % of silsesquioxane was investigated by FTIR, TGA, scanning electron microscopy (SEM), X-ray diffraction (XRD), and DMA techniques. FTIR spectra shows the existence of hydrogen bonding in the PU-POSS system. The intensity of hydrogen bonding decreases with the increase in POSS-H loading suggesting the prevention of the formation of hydrogen bonding by the addition of POSS-H molecule. SEM analysis reveals the incompatibility of POSS-H molecule in the PU matrices exhibiting greater extent of phase separation and a large number of POSS aggregates on the addition of POSS-H molecule in the PU-POSS matrices. The TGA thermograms show that the POSS-PU hybrids possess excellent thermal stabilities. However, the incorporation of POSS-H molecule leads to a decrease in the thermal properties and only the char yield values increase with the increase in the POSS-H content in the PU-POSS hybrids. The XRD pattern reveals that the crystalline structure of POSS molecules are destroyed by the polymer matrices in the PU-POSS hybrid films. The decrease in the bending storage modulus E' values with the increase in the POSS-H content proves the retardation of hydrogen bonding formation by the POSS-H molecule in the PU-POSS hybrid. © 2009 Wiley Periodicals, Inc. J Appl Polym Sci 114: 3659–3667, 2009

Key words: polyurethane; thermal; mechanical; morphology; nanocomposites

INTRODUCTION

Polyurethanes (PUs) are multiblock copolymers usually consisting of hard and soft segments. The hard segments are based on diisocyanate and/or chain extenders, whereas the soft segments are polyether, polyester, or polydimethylsiloxane (PDMS).[1–3] The incompatibility between the hard and soft segments exhibits a larger extent of phase separations in the PU bulk polymer. The extent of phase separation and the various chemical structures of the hard and soft segments of PU exhibit interesting mechanical properties.[4] PUs are widely used as membranes, adhesives, coatings, and in biomedical applications such as artificial heart valve and microvessels.[5–8] However, the typical PUs known to have small resistance to heat is the main reason for limiting the application of PUs.

Correspondence to: B. S. R. Reddy (induchem2000@yahoo.com).

Contract grant sponsor: Department of Science and Technology, New Delhi; contract grant number: SR/S1/PC-33/2006.

There are many accepted approaches for the improvement of thermal stability of PUs. One of the important approaches is the chemical modification of its structure by blending or copolymerizing with more thermally stable polymers such as PDMS[9] or polyimide (PI).[10] However, the incorporation of PDMS leads to a decrease in the mechanical properties, whereas PI imparts poor solubility. Also, the difficulty in processing techniques limits the usage of PI and PDMS in PUs. The other way of solving this problem is to modify the thermal and mechanical properties of PU by blending nanoparticles into the thin films of diblock copolymers of PU using ZnO nanoparticle. However, the nanoparticles having controlled and well-defined surfaces are needed to control the properties of block copolymers.[11]

Recently, polyhedral oligomeric silsesquioxane (POSS) blocks emerged as a new class of nanofillers for high-performance hybrids with improving thermal and mechanical properties.[12–14] POSS is a class of important nanosized (1–3 nm) and cagelike molecules derived from the hydrolysis and condensation of trifunctional organosiloxanes. POSS molecules possess a formula of $[RSiO_{3/2}]n$, where n is 6–12 and R can be various types of organic groups, one (or more) of which is reactive or polymerizable

functional groups. Polymers incorporated with well-defined nanosized POSS cages represent a class of important organic–inorganic nanocomposites.[15] POSS can also be incorporated into the polymer matrix either by blending or chemically reacting POSS molecule with the reactive monomers or polymer precursors. In both cases, the POSS molecules undergoes self-aggregation by competing with both chemical bonding and molecular dispersion in the matrix.[16] Morphology and phase separation plays a major role in the properties of the nanocomposites. Although individual POSS molecules are, themselves, nanometer-sized fillers, materials with molecular POSS dispersion are expected to have different properties than those containing nanometer-sized aggregates or microsized particles.[17] Organic/inorganic materials prepared using POSS have been found to offer attractive properties that include increased thermal, oxidation stability, high UV stability, chemical resistance, decreased flammability, and enhanced mechanical properties.[18] The reduced shrinkage properties of POSS-incorporated nanocomposites are used as dental destrotive materials.[19] A very few research works were reported on PU's incorporated POSS macromer because functionalization of POSS macromer to form PU nanocomposite is difficult. Neumann et al.[20] synthesized PU network using isocyanate-functionalized POSS cage and polyethylene glycol. Liu and Zheng[21] and Liu et al.[22] used amine- and hydroxyl-functionalized POSS cages for the synthesis of PU-POSS nanocomposite. Fu et al.[23,24] synthesized POSS group pendant to PU chain. Recently, Oaten and Choudhury[25] synthesized a POSS-urethane hybrid using isobutyltrisilanol POSS with hexamethylene diisocyanate (HDI) and they have shown that the POSS incorporation improves the thermal and mechanical stability of thin PU hybrid films.

In this work, we have used a partially caged heptacyclopentyl tricycloheptasiloxane triol (CyPOSS), fully caged octakis(hydridodimethylsiloxy)octasilsesquioxane (POSS-H), hydroxyalkyl terminated PDMS, and HDI to obtain PU-POSS hybrid film. The main focus of this work is to study how the partially or the fully caged silsesquioxane will affect the thermal properties, compatibility, morphology, and the mechanical properties of the POSS-incorporated PU networks. For this purpose, the thermal and the microstructures of PU networks were characterized by TGA, scanning electron microscopy (SEM), and X-ray diffraction (XRD), and the mechanical properties was characterized using DMA techniques.

EXPERIMENTAL

Materials and measurements

Poly(dimethylsiloxane) bis(hydroxylalkyl) terminated (M_n) 5600 (PDMS, Aldrich, St. Louis, MO), trichlorocyclopentylsilane, tetraethoxy silane (Aldrich), tetramethyl-ammonium hydroxidepentahydrate (Aldrich), chlorodimethyl silane (Aldrich), HDI (Merck, India), and di-*n*-butyl tin dilaurate (DBTDL, Merck) were used as received. Hexane, methanol, acetonitrile, and tetrahydrofuran (THF) were used as received, and toluene was dried over calcium hydride.

IR spectra were recorded using Perkin-Elmer FTIR Spectrometer using KBr pellet technique. ^{1}H-, ^{13}C-, and ^{29}Si-NMR spectra were recorded using $CDCl_3$ and THF (for CyPOSS) as a solvent and TMS as an internal standard on JEOL 500 MHz.

Thermogravimetric analyses were performed at a scanning rate of 10°C/min under N_2 atmosphere with a TGA Q50- TA instrument.

Dynamical mechanical (DMA) tests were carried out under N_2 atmosphere by means of NETZSCH DMA 242 mechanical analyzer on samples of following sizes 25 : 5: 0.5 mm at 0.1 Hz frequencies and the temperature range of −110–250°C, with a heating rate of 5°C.

The bulk morphology of the hybrid films were analyzed by SEM using Jeol 400 Microscope. The films were cut into pieces and the SEM pictures were taken on the flat surfaces.

The microstructures of the hybrid films were analyzed by wide-angle X-ray diffraction (WAXD) measurements. The diffractograms were obtained from Seifert Jso-Debyeflex-2002 instrument in normal/transmission mode with Ni-filtered Cu Kα radiation (1.54 Å wavelength). Data were obtained with the incident beam normal to the plane of the film.

Synthesis of heptacyclopentyl tricycloheptasiloxane triol (CyPOSS)

Heptacyclopentyl tricycloheptasiloxane triol was synthesized using reported literature procedure.[26] 37.5 mL of acetonotrile was placed in a 100-mL three-necked RB flask, and then 1.4 mL of cyclopentyl trichlorosilane was added. To this, 9.4 mL of deionized water was carefully added to the reaction mixture (Scheme 1). The homogeneous solution was vigorously stirred and heated under reflux condition in an oil bath kept at 90°C. After 3 h, a white precipitate was observed on the sides of the RB flask and the reaction was carried out for 12 h. Then, the white precipitate present on the walls of the flask were separated and washed with acetonitrile and water repeatedly. Then the precipitate was redissolved in THF and precipitated in acetonitrile. A white precipitate was obtained (yield 55%).

IR (cm^{-1}): 3409 (Si—OH stretch), 2949 (C—H stretch), 1107 (Si—O—Si stretch); ^{1}H-NMR: (500 MHz, THF): 3.0 ppm (—Si—OH), 1.97 ppm (—CH_2—CH_2—CH—Si—), 1.78 ppm (—CH_2—CH—Si—), and 1.18 ppm (*CH*—Si—); ^{13}C-NMR (500 MHz, THF):

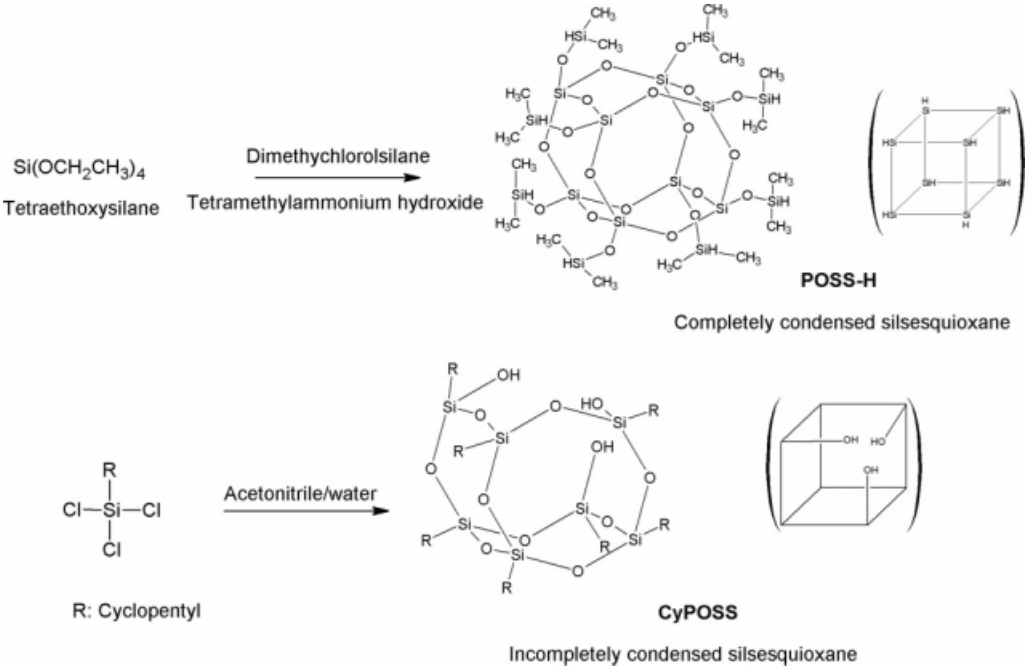

Scheme 1 Synthesis of POSS-H and CyPOSS monomers.

27.64 ppm (—CH_2—CH_2—CH—Si), 23.41(CH_2—CH—Si—), and 23.00 ppm (—CH—Si—); ^{29}Si-NMR (500 MHz, THF): 57.29 ppm for —Si—OH, and 66.66 and 65.07 ppm for (—Si—$(O)_4$).

Synthesis of octakis(hydridodimethylsiloxy) octasilsesquioxane (POSS-H)

The synthesis of octakis(hydridodimethylsiloxy)octasilsesquioxane[27] (POSS-H) from a solution of tetramethylammonium silicate, which was prepared by adding 2.5 g (25%) of tetramethylammonium hydroxide in 10 mL of methanol and 3.64 mL of distilled water to 5.32 mL of tetraethoxy silicate. The resulting solution was stirred for 24 h at room temperature and was added dropwise to a mixture of chlorodimethyl silane (4 mL), hexane (60 mL), and 10 mL of methanol solution. The mixture was stirred for 4 h. The two phases formed were separated, and the hexane solution was removed in vacuum to give a white solid. The solid was washed with methanol and dried in vacuum at 80°C for 4 h (yield 50%).

IR (cm^{-1}): 2145 (Si—H stretch), 1261 (Si—$(CH_3)_2$), 1100 (Si—O—Si stretch), and 904 (Si—H rocking); ^{1}H-NMR (500 MHz, $CDCl_3$): 4.72 ppm (Si—H) and 0.26 ppm (Si—CH_3); ^{13}C-NMR (500 MHz, $CDCl_3$): 0.12 ppm (Si—CH_3); ^{29}Si-NMR (500 MHz, $CDCl_3$): −3.95 ppm (—Si—H) and −112.48 ppm for ($Si(O)_4$).

Synthesis of PU-POSS hybrid nanocomposites

HDI was dissolved in 10 mL of dry toluene under nitrogen atmosphere in a 100-mL three-necked flask. To this, predetermined amount of PDMS, CyPOSS, and POSS–H were dissolved in 20 mL of toluene and then added at 60°C. Then 1–2 drops of DBTDL catalyst was added, and the reaction mixture was stirred vigorously for 6 h. Finally, the reaction mixture was poured into the Teflon-coated petridish and kept for curing at room temperature. To prevent dust pollution, the top of the glass plate was covered with a filter paper and the hybrid film was peeled out from the glass plate and dried at 80°C in the atmospheric air for 48 h.

RESULTS AND DISCUSSION

Synthesis and characterization of PU-POSS hybrid nanocomposites

Several different chemical compositions of HDI, PDMS, POSS–H, and Cy-POSS were reacted in the presence of DBTDL as a catalyst to obtain PU-POSS hybrid films. Their chemical compositions are shown in Table I. The functional groups of the monomer in the model reaction and the chemical structure of the

TABLE I
Various Chemical Compositions of PU-PDMS Hybrid Nanocomposites

S.No.	Sample	PDMS (wt %)	HDI (wt %)	CyPOSS (wt %)	POSS-H (wt %)
1	PU-POSS-1	70	20	10	–
2	PU-POSS-2	70	17.5	10	2.5
3	PU-POSS-3	70	15	10	5
4	PU-POSS-4	70	12.5	10	7.5

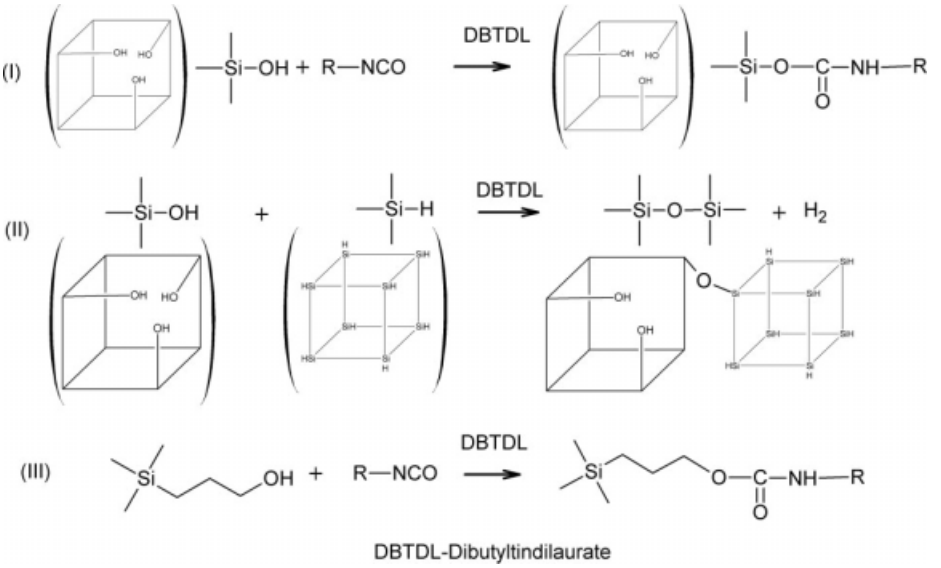

Scheme 2 Model reaction of the monomerfunctional groups.

crosslinked PU-POSS hybrid films are shown in Schemes 2 and 3. The model reaction of the monomer (Scheme 2) clearly depicts the possible reaction of the monomer functional sites in the presence of DBTDL as a catalyst. In this work, we have tried to incorporate both completely condensed POSS and incompletely condensed CyPOSS into the PU matrices. Therefore, we have chosen the incompletely condensed CyPOSS molecule with a hydroxyl functional group to form urethane linkage with the isocyanate group. On the other hand, the hydride functional group in the completely condensed POSS-H molecule reacts with the hydroxyl functional group of incompletely condensed CyPOSS molecule in the presence same DBTDL catalyst. The hybrid films synthesized were characterized using FTIR. The FTIR spectrum of PU-POSS hybrid films and the POSS macromers used for the synthesis of

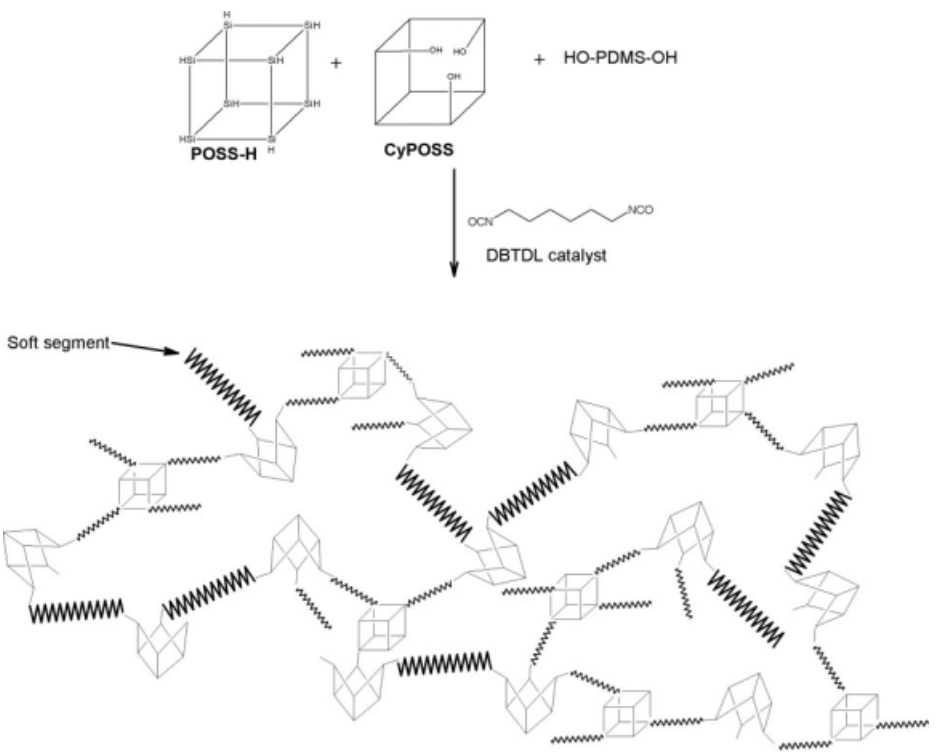

Scheme 3 Chemical structure of PU-POSS hybrid nanocomposites.

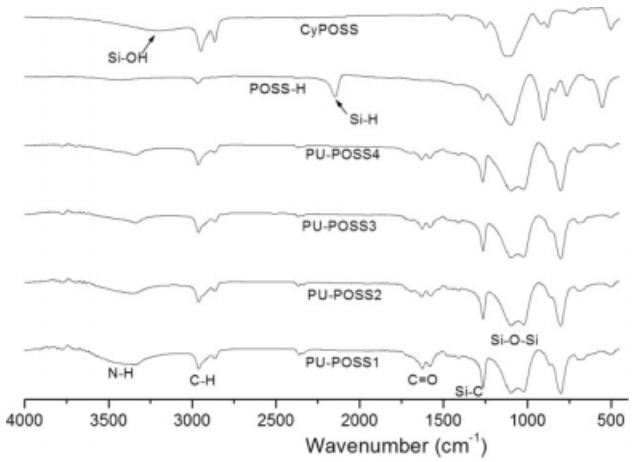

Figure 1 FTIR spectrum of CyPOSS, POSS-H macromers, and PU-POSS hybrid nanocomposites.

nanohybrids are shown in Figure 1. Based on the synthetic procedure (Scheme 3) of the PU-POSS nanocomposites, two basic questions can be arised: (i) whether the isocyanate groups reacted completely with hydroxyl group of CyPOSS molecule to form a CyPOSS-urethane linkages and (ii) Si—H group of the POSS-H reacted completely with hydroxyl group of CyPOSS molecule to form CyPOSS-POSS linkage in the presence of DBTDL catalyst. Since FTIR technique is an excellent tool to determine the chemical structure of PU hybrids, by using IR technique these two questions can be answered almost quantitatively. The characteristic band at 2270 cm^{-1} represents the isocyanate group, which completely disappeared in the IR spectrum of all the PU-POSS hybrid films, confirming that all the isocyanate molecules completely reacted with the hydroxyl group of CyPOSS and hydroxyl group of PDMS chain. On the other hand, the Si—H of POSS band near 2100 cm^{-1} also completely disappeared for all the PU-POSS films. The FTIR spectrum of completely condensed POSS monomer, when compared with, is shown in Figure 1. We have anticipated the incomplete Si—H condensation reaction with Si—OH in the presence of DBTDL catalyst because of the bulkiness of the POSS molecule. However in this case, surprisingly, all the POSS completely reacted and formed CyPOSS-POSS linkage, showing the complete distribution of POSS in the PU-POSS nanocomposites. The band near 1627 cm^{-1} shows the formation of (C=O) urethane linkage with hydroxyl group of PDMS and CyPOSS. A very broad band near 3341 cm^{-1} corresponds to hydrogen-bonded N—H urethane linkage, which confirms the existence of hydrogen bond formation between the urethane linkages. The broad band of urethane representing the hydrogen bonding decreases with the incorporation of POSS-H molecule in the PU-POSS-2, PU-POSS-3, and PU-POSS-4 hybrids. This implies that the incorporation of POSS-H molecule retards the formation of hydrogen bonds between the urethane linkages. The prediction of Si—OH completion is quite complicated by the fact that the Si—OH band overlaps with the hydrogen-bonded N—H urethane band near 3341 cm^{-1}. The IR spectrum of PU-POSS hybrid shows two bands at 1104 and 1013 cm^{-1} corresponding to the Si—O—Si linkage of the POSS cubic structure and Si—O—Si linkage of the PDMS straight chain. The band at 1104 cm^{-1} (Si—O—Si cube) was observed in all the PU-POSS films, which suggests that the POSS cube has remained intact during the nanocomposite formation.

Thermogravimetric analysis

The thermal stabilities of the PU-POSS hybrids were characterized with TGA under N_2 atmosphere. The initial decomposition for all the PU-POSS are similar and the initial decomposition (5 wt %) starts at 275°C for all the PU-POSS hybrids, showing excellent thermal stability when compared with POSS-free PU hybrids (Fig. 2). The decrease in the thermal properties was observed for PU-POSS hybrid films on increasing the addition of completely condensed POSS group. The CyPOSS-substituted hybrid shows a very high thermal stability because of the presence of thermally stable cyclopentyl group in the vertices of CyPOSS group and the formation of more hydrogen bonding when compared with methyl substitution in the POSS-H group. Incorporation of 2.5 wt % of completely condensed POSS-H into the PU-POSS matrices shows more decrease in thermal properties of the PU-POSS-2 hybrid film. On further increasing the POSS-H incorporation, thermal properties slightly increases for the hybrids as shown in PU-POSS-3 and PU-POSS-4. However, the improved thermal properties of these hybrids are quite low

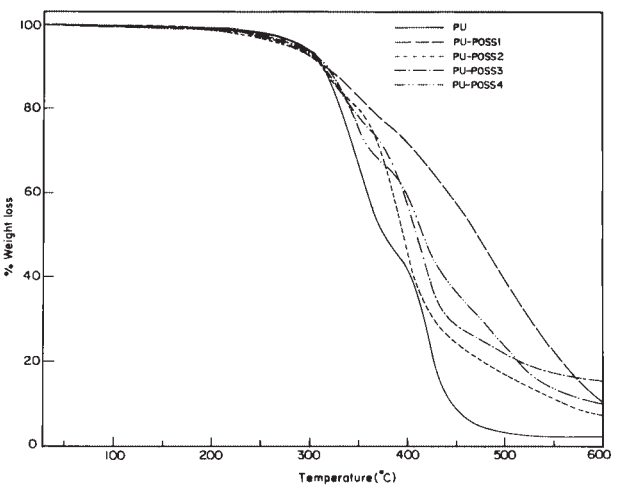

Figure 2 TGA curves of PU-POSS hybrid nanocomposites.

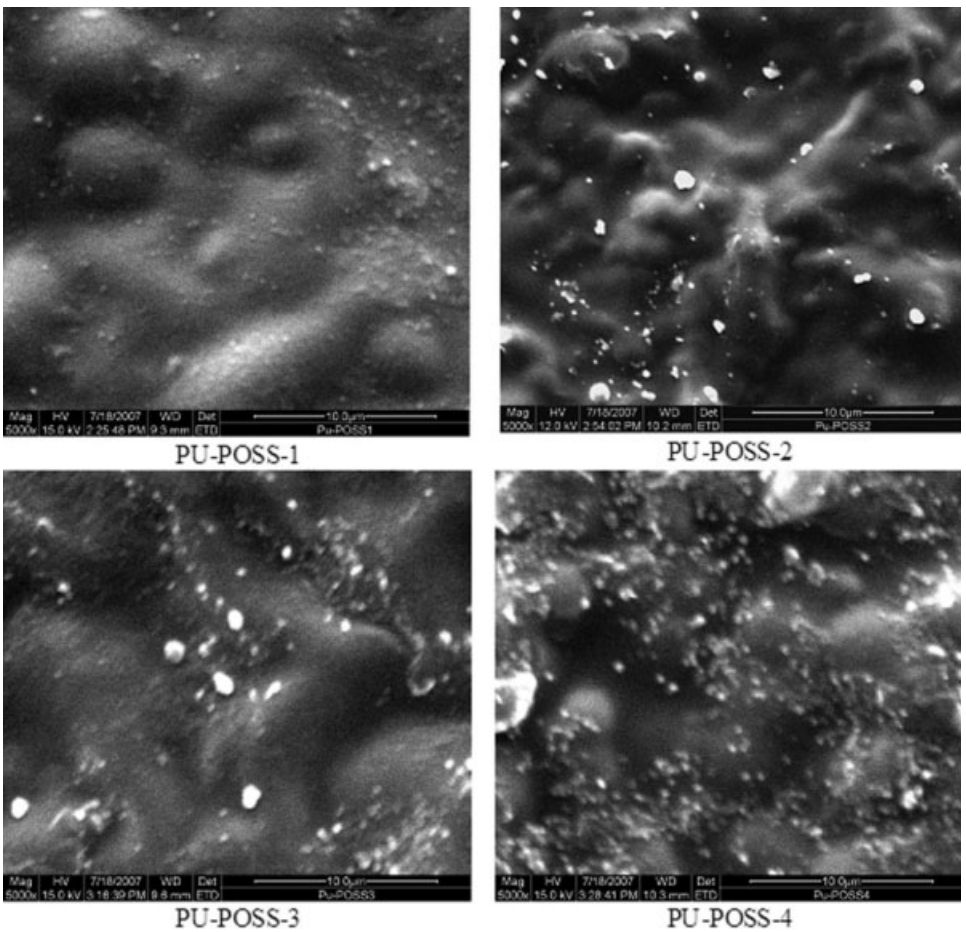

Figure 3 SEM images of PU-POSS hybrid nanocomposites.

when compared with PU-POSS-1 hybrid film. The mixed completely condensed POSS and incompletely condensed POSS-incorporated PU-POSS hybrids (PU-POSS-2, PU-POSS-3, and PU-POSS4) show two-stage decomposition and the incompletely condensed POSS-incorporated hybrid (PU-POSS-1) shows single-stage decomposition in the TGA thermograms. These observations indicate that the completely condensed POSS molecule relatively affects the thermal properties of PU-POSS hybrids even at lower concentration. The two-stage decomposition shows the presence of various domains of CyPOSS-POSS and CyPOSS-urethane aggregates in the polymer matrices. As we have discussed previously, the initial decomposition for all the PU-POSS hybrids are similar and this may be due to the decomposition of thermally less stable urethane group. The second-stage decomposition observed for PU-POSS-2, PU-POSS-3, and PU-POSS-4 hybrids near 366°C were due to the stable PDMS chain, which was not observed in the PU-POSS-1. The final residue for PU-POSS-1 and POSS-2 hybrids at 700°C remains the same, whereas it increases for the PU-POSS-3 and PU-POSS-4 hybrids with increase in the concentration of completely condensed POSS. This clearly shows that the POSS-H aggregates remain unaltered even at 700°C, but the contribution of completely condensed POSS-H for the polymer matrices as a whole in thermal properties is very less. The high thermal properties of PU-POSS-1 hybrid make us believe that the nature of the POSS group, reactive functional group in the POSS, and the rigid bulky group on the vertices of the POSS are the three main factors required for the modification of the thermal properties of nanocomposites.

Scanning electron microscopy analysis

Figure 3 displays SEM images of the bulk morphology of PU-POSS-1, PU-POSS-2, PU-POSS-3, and PU-POSS-4 hybrid films. All the PU-POSS films show a microphase separation of urethane hard segments and a micro/nanolevel spheroidical aggregation of POSS-rich domains. Similar observations were reported[17] about the aggregation of POSS from nano to microlevel, and the hydrogen bonding increases the compatibility in the phenolic reisn–POSS hybrid nanocomposites. It can be clearly seen in the SEM images that the POSS aggregates into POSS-rich spheroidical domains in the PU-POSS hybrid films.

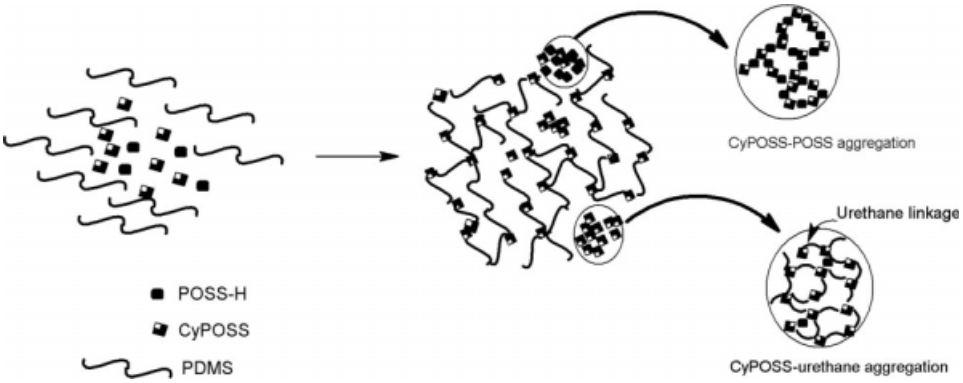

Figure 4 Schematic representation of POSS aggregations in PU-POSS hybrid nanocomposites.

The schematic representation of POSS aggregation in the PU-POSS matrices is shown in Figure 4. However, the type of aggregation of POSS groups and the phase separation in all the films are different. There was an excellent dispersion of CyPOSS-urethane aggregates in the PU-POSS-1 film. The aggregations are inhomogeneous in the case of PU-POSS-2, PU-POSS-3, and PU-POSS-4 films and are highly phase-separated from the polymer matrix. The excellent dispersion of CyPOSS-urethane aggregates in the PU-POSS-1 is explained by the combination of three factors. (i) The reactivity of trisilanol group with isocyanate so that it can incorporate CyPOSS evenly in the network, during the early stage of the polymerization. (ii) The high compatibility of CyPOSS in the PU matrices rather than completely condensed POSS-H, where the CyPOSS interacts highly with the polymer matrices. (iii) The possibility for favorable CyPOSS-CyPOSS organization in the PU matrices. The combination of these three factors creates a homogeneous aggregation of CyPOSS-urethane and even distribution of aggregates in the polymer matrices. The hybrids PU-POSS-2, PU-POSS-3, and PU-POSS-4 show a large fraction of POSS aggregation and inhomogeneous aggregations. This may be due to the formation of hydrophobic CyPOSS-POSS aggregates, which are having less interaction with polymer matrices. The fraction of POSS aggregation increases with increasing the addition of completely condensed POSS-H cage structure.

Dynamical mechanical analysis

The bending storage modulus E' versus temperature curves at 0.1 Hz for PU-POSS hybrids are shown in Figure 5. The decrease in the storage modulus with increase in the concentration of completely condensed silsesquioxane was observed. The storage modulus of PU-POSS-1 is higher than the mixed CyPOSS and POSS hybrid films such as PU-POSS-2, PU-POSS-3, and PU-POSS-4. This is due to the CyPOSS-urethane interaction with polymer matrix and the formation of hydrogen bonding in the case of PU-POSS-1. The decrease in the storage modulus of PU-POSS-2, PU-POSS-3, and PU-POSS-4 may be due to the formation of hydrophobic CyPOSS-POSS aggregates in the matrices, which in turn reduces the interchain interactions and interrupts the PU-hydrogen bonding formation. As seen in the SEM analysis, PU-POSS-2, PU-POSS-3, and PU-POSS-4 hybrids exhibit more aggregation and are all highly phase-separated from the polymer matrix because of the hydrophobic nature of CyPOSS-POSS aggregation in the matrix. All these factors suggest that the contribution of POSS cage structure alone may not be enough to improve the mechanical properties; however, the cage interaction with the polymer matrix and their functional groups are all highly dependent.

The loss factor tan δ is the ratio of the loss modulus to the storage modulus and is very sensitive to the structural transformation of the material. The tan

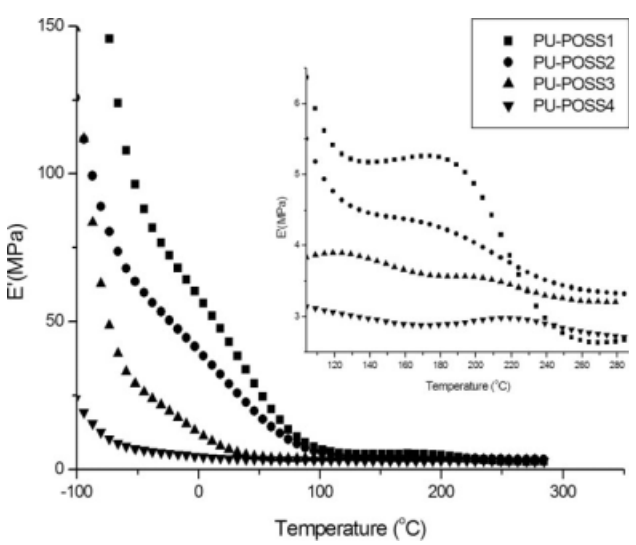

Figure 5 The storage modulus (E') versus temperature curves of PU-POSS hybrid nanocomposites.

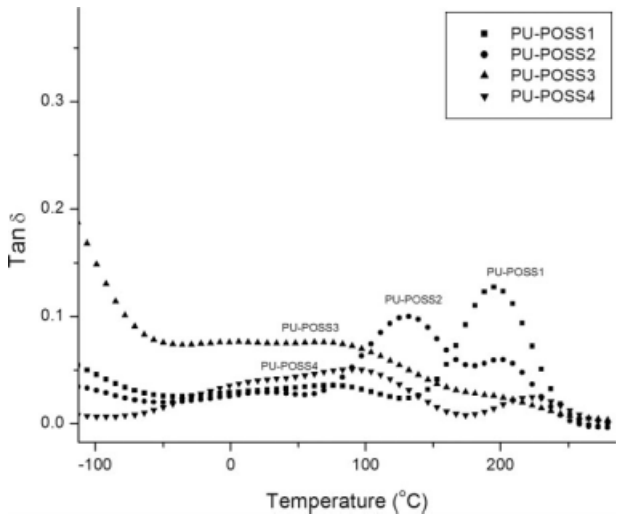

Figure 6 The tan δ versus temperature curves of PU-POSS hybrid nanocomposites.

δ versus temperature curves for the PU-POSS hybrids are shown in Figure 6. The tan δ peak can be used to identify T_g of these nanocomposites. Generally, the T_g value of polymer-POSS hybrid depends on the nature of the interactions of the POSS cages with the polymer matrix, namely functionalities of POSS, the types of polymer matrices, and the organic groups in the POSS vertices. The other three competitive factors that affect the T_gs are as follows: (i) the dispersion of POSS cages at the molecular level could restrict the motion of the macromolecular chains, which would enhance T_g; (ii) the inclusion of bulky POSS group increases the free volume of the system, which would result in the depression of T_g; (iii) the inclusion of POSS cage could act like a plasticizer by interrupting the formation of hydrogen bonding between the polymer matrices and suppresses the T_g of the hybrids. The height and the broad width of the tan δ peak for the PU-POSS-1 hybrid film suggests the homogeneous distribution of CyPOSS molecule in the PU-POSS matrices and show a single tan δ peak (T_g at 194°C). The tan δ peaks for the PU-POSS-2, PU-POSS-3, and PU-POSS-4 hybrid films are suppressed and show two peaks. As we have discussed earlier, there were two different types of aggregations arising from the CyPOSS-urethane and CyPOSS-POSS. These two different types of aggregates occupy various domains of the polymer matrices. The very high interaction between polymer matrices and the CyPOSS-urethane aggregates shows very high T_g and the less interaction CyPOSS-POSS aggregates with the polymer matrices showing lower T_g. This type of behavior is clear and is in good agreement with SEM analysis. The large number of aggregates of CyPOSS-POSS reduces the hydrogen bonding involved in the polymer matrices and thereby reduces the T_g of the hybrid. From the DMA analysis, we can suggest that the CyPOSS-POSS and CyPOSS-urethane spheroidical aggregates occupies into separate domains in the polymer matrices because of the incompatibility of POSS-H cages with PU matrices. The lower T_g values at 129, 98, and 93°C for PU-POSS-2, PU-POSS-3, and PU-POSS-4, respectively, are due to the restriction of PU matrices by the CyPOSS-POSS aggregates. The higher T_gs, 197, 191, and 220°C for PU-POSS-2, PU-POSS-3, and PU-POSS-4, respectively, are due to the restriction of PU matrices by the CyPOSS-urethane aggregates.

Wide-angle x-ray diffraction

The microstructure of PU-POSS hybrids is of further interest to be studied by the WAXD measurements. Figure 7 displays XRD patterns of PU-POSS hybrids. For comparison, the diffraction patterns of pure CyPOSS and POSS-H are also shown. The pure Cy-POSS and POSS-H molecule shows crystalline peaks at $2\theta = 7.0°$, 10.2°, 11.5°, and 18.3°. All the crystalline peaks of Cy-POSS and POSS-H peaks are absent in the PU-POSS hybrid films. This implies that the crystallinity of POSS molecules were collapsed by the polymer matrices in the PU-POSS hybrids. A broad peak at $2\theta = 11.3°$ in all the hybrids was observed, which may be due to the amorphous nature of the PDMS matrices. These observations could reflect that there is an absence of crystalline microdomains in the POSS-rich phase and also confirms the absence of macrolevel POSS aggregation in the PU-POSS hybrids.

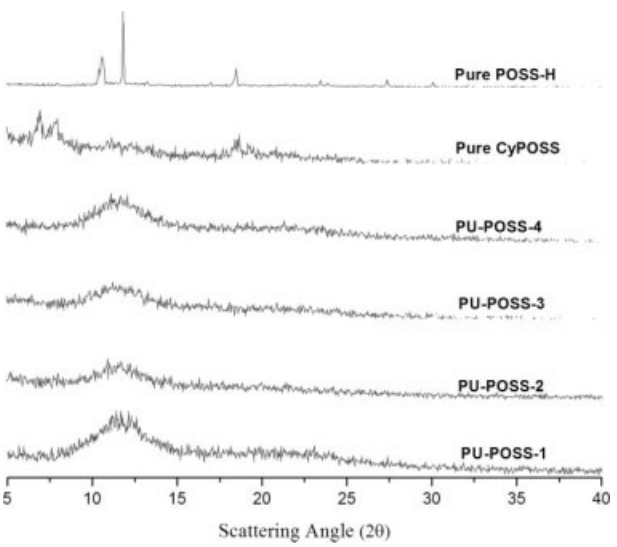

Figure 7 XRD patterns of POSS-H, CyPOSS macromers, and PU-POSS hybrid nanocomposites.

CONCLUSION

A series of PU-POSS hybrids consisting of various compositions of completely condensed and incompletely condensed POSS were synthesized. The morphology and the mechanical properties of hybrids are highly affected by the completely condensed POSS-H molecule. The completely condensed POSS-H molecule forms nano/microlevel spheroidical aggregates with incompletely condensed CyPOSS molecule. These aggregates retard the formation of hydrogen bonding between the polar urethane linkages. The mechanical and thermal properties are highly suppressed by the formation of these aggregates since these aggregates act like spacers between the polymer chains because of their incompatible nature with the PU-POSS matrices. An absence of crystalline microdomains arising from the POSS molecule in PU-POSS hybrids was observed. The crystallinty of these POSS molecules are destroyed by the interaction of polymer matrices in the PU-POSS hybrids. The overall conclusion drawn from all the observations is that the rigid POSS cubic-cage structure alone is not imparting the properties to the bulk polymer but also the functional group, compatibility of the POSS molecule with the polymer matrices, and bulky substituents in the vertices of the POSS molecules alters the bulk properties of the polymers.

Mr. K. Madhavan thanks CSIR for the senior research fellowship.

References

1. Chen, R. S.; Chang, C. J.; Chang, Y. H. J Polym Sci Part A: Polym Chem 2005, 43, 3482.
2. Stanciu, A.; Airinei, A.; Oprea, S. Polymer 2001, 42, 6081.
3. Sonnenschein, M. F.; Lysenko, Z.; Brune, D. A.; Wendt, B. L.; Schrock, A. K. Polymer 2005, 46, 10158.
4. Furukawa, M.; Mitsui, Y.; Fukumaru, T.; Kojio, K. Polymer 2005, 46, 10817.
5. Jena, K. K.; Chattopadhyay, D. K.; Raju, K. V. S. N. Eur Polym J 2007, 43, 1825.
6. Madhavan, K.; Reddy, B. S. R. J Membr Sci 2006, 283, 357.
7. Bernacc, G. M.; Connor, B. O.; Williams, D. F.; Wheatley, D. J. Biomaterials 2002, 23, 45.
8. Kannan, R. Y.; Salacinski, H. J.; Edirisinghe, M. J.; Hamilton, G.; Seifalian, A. M. Biomaterials 2006, 27, 4618.
9. Wang, L. F.; Ji, Q.; Glass, T. E.; Ward, T. C.; McGrath, J. E.; Muggli, M.; Burns, G.; Sorathia, U. Polymer 2000, 41, 5083.
10. Yeganeh, H.; Shamekhi, M. A. Polymer 2004, 45, 359.
11. Zheng, J.; Ozisik, R.; Siegel, R. W. Polymer 2005, 46, 10873.
12. Cheng, C. F.; Cheng, H. H.; Cheng, P. W.; Lee, Y. J. Macromolecules 2006, 39, 7583.
13. Nanda, A. K.; Wicks, D. A.; Madbouly, S. A.; Otaigbe, J. U. Macromolecules 2006, 39, 7037.
14. Drazkowski, D. B.; Lee, A.; Haddad, T. S. Macromolecules 2007, 40, 2798.
15. Ni, Y.; Zheng, Z. J Polym Sci Part A: Polym Chem 2007, 45, 1247.
16. Liang, K.; Li, G.; Toghiani, H.; Koo, J. H.; Pittman, C. U., Jr. Chem Mater 2006, 18, 301.
17. Zhang, Y.; Lee, S.; Yoonessi, M.; Liang, K.; Pittman, C. U. Polymer 2006, 47, 2984.
18. Mya, K. Y.; He, C.; Huang, J.; Xiao, Y.; Dai, J.; Siow, Y. P. J Polym Sci Part A: Polym Chem 2004, 42, 3490.
19. Soh, M. S.; Yap, A. U. J.; Sellinger, A. Eur Polym J 2007, 43, 315.
20. Neumann, D.; Fisher, M.; Tran, L.; Matisons, J. G. J Am Chem Soc 2002, 124, 13998.
21. Liu, H.; Zheng, S. Macromol Rapid Commun 2005, 26, 196.
22. Liu, Y.; Ni, Y.; Zheng, S. Macromol Chem Phys 2006, 207, 1842.
23. Fu, B. X.; Hsiao, B. S.; Pagola, S.; Stephens, P.; White, H.; Rafailovich, M.; Sokolov, J.; Mather, P. T.; Jeon, H. G.; Phillips, S.; Lichtenhan, J.; Schwab, J. Polymer 2001, 42, 599.
24. Fu, B. X.; Hsiao, B. S.; White, H.; Rafailovich, M.; Mather, P. T.; Jeon, H. G.; Phillips, S.; Lichtenhan, J.; Schwab, J. Polym Int 2000, 49, 437.
25. Oaten, M.; Choudhury, N. M. Macromolecules 2005, 38, 6392.
26. Pescarmona, P. P.; Raimondi, M. E.; Tetteh, J.; McKay, B.; Maschmeyer, T. J Phys Chem A 2003, 107, 8885.
27. Choi, J.; Yee, A. F.; Laine, R. M. Macromolecules 2003, 36, 5666.